
EFDA–JET–CP(03)03-14

D. Van Eester, F. Imbeaux, P. Mantica, M. Mantsinen, M. de Baar, P. de Vries,
L.-G. Eriksson, R. Felton, A. Figueiredo, J. Harling, E. Joffrin, K. Lawson,
H. Leggate, X. Litaudon, V. Kiptily, J.-M. Noterdaeme, V. Pericoli,
E. Rachlew, A. Tuccillo, K.-D. Zastrow and JET EFDA Contributors

Recent ^3He Radio Frequency Heating Experiments on JET

Recent ^3He Radio Frequency Heating Experiments on JET

D. Van Eester¹, F. Imbeaux², P. Mantica³, M. Mantsinen⁴, M. de Baar⁵,
P. de Vries⁶, L.-G. Eriksson², R. Felton⁶, A. Figueiredo⁷, J. Harling⁶, E. Joffrin²,
K. Lawson⁶, H. Leggate⁶, X. Litaudon², V. Kiptily⁶, J.-M. Noterdaeme^{8,9},
V. Pericoli¹⁰, E. Rachlew¹¹, A. Tuccillo¹⁰, K.-D. Zastrow⁶
and JET EFDA Contributors*

¹LPP-ERM/KMS, Association "EURATOM – Belgian State", TEC, Brussels, Belgium

²Association EURATOM-CEA, CEA-Cadarache, Saint-Paul-Lez Durance, France

³Instituto di Fisica del Plasma, EURATOM-ENEA-CNR Association, Milan, Italy

⁴Helsinki University of Technology, Association EURATOM-Tekes, Finland

⁵FOM-Rijnhuizen, Associatie EURATOM-FOM, TEC, Nieuwegein, The Netherlands

⁶EURATOM/UKAEA Fusion Association, Culham Science Centre, Abingdon, United Kingdom

⁷Associação EURATOM-IST, Centro de Fusão Nuclear, Lisboa, Portugal

⁸Max-Planck IPP-EURATOM Assoziation, Garching, Germany

⁹Gent University, EESA Department, B-9000 Gent, Belgium

¹⁰Associazione EURATOM-ENEA sulla Fusione, CR Frascati, Rome, Italy

¹¹KTH Association EURATOM/VR, SE-10044 Stockholm, Sweden

* See annex of J. Pamela et al, "Overview of Recent JET Results and Future Perspectives", Fusion Energy 2000 (Proc. 18th Int. Conf. Sorrento, 2000), IAEA, Vienna (2001).

Preprint of Paper to be submitted for publication in Proceedings of the
15th Topical Conference on Radio Frequency Power in Plasmas
(Moran, Wyoming, USA 19-21 May 2003)

“This document is intended for publication in the open literature. It is made available on the understanding that it may not be further circulated and extracts or references may not be published prior to publication of the original when applicable, or without the consent of the Publications Officer, EFDA, Culham Science Centre, Abingdon, Oxon, OX14 3DB, UK.”

“Enquiries about Copyright and reproduction should be addressed to the Publications Officer, EFDA, Culham Science Centre, Abingdon, Oxon, OX14 3DB, UK.”

ABSTRACT.

Various ITER relevant experiments using ^3He in a majority D plasma were performed in the recent JET campaigns. Two types can be distinguished: dedicated studies of the various RF heating scenarios which rely on the presence of ^3He , and physics studies using RF heating as a working tool to provide a tunable heat source. As the success of a number of these experiments depended on the capability to keep the ^3He concentration fixed, real time control of the ^3He concentration was developed and used. This paper presents a brief overview of the results obtained, zooms in on some of the more interesting recent findings and discusses some of the theoretical background.

1. INTRODUCTION

One of the advantages of Radio Frequency (RF) heating in tokamaks is linked to the fact it is based on resonant and thus localized wave-particle interaction at the position where $\omega = k_{\parallel}v_{\parallel} + N\Omega(\bar{x})$ is satisfied (see e.g. [1,2]). Here ω is the antenna frequency, k_{\parallel} is the projection of the wave vector of the electromagnetic wave on the confining magnetic field $\bar{B}_o(\bar{x})$, v_{\parallel} is the parallel velocity and Ω is the cyclotron frequency. Via a proper choice of the ratio of ω and B_o one can therefore deposit power at specific desired radial positions. At small concentrations of the minority gas, efficient ion heating can be achieved at $\omega \approx \Omega$ while at harmonics of the majority gas ($\omega \approx N\Omega$; $N > 1$) finite Larmor radius effects allow direct heating of a subpopulation of the bulk ions. Whereas electron Landau or TTMP damping at $\omega = k_{\parallel}v_{\parallel}$ on the externally via RF antennae excited fast wave often gives rise to rather broad electron power deposition profiles, electron absorption on the short wavelength Bernstein wave branch to which the fast wave converts at the ion-ion hybrid layer is much more localized.

In ^3He -D plasmas, efficient single pass direct ^3He minority heating requires a small ^3He concentration of 3-5 percent while efficient mode conversion, on the contrary, necessitates a large concentration of 15-20%. As the mode conversion position is a known function of the concentration, the mode conversion position can be fixed at a desired location by controlling the concentration. A proper choice of the concentration and ω/B_o therefore not only decides on which direct heating (i or e) is preferred but also at which radial position it takes place.

There are various reasons for examining shots involving ^3He . Firstly, performing discharges using ^3He as a minority allows studying basic RF physics. As the presence of a small RF heated ^3He minority enhances the fusion reactivity in ITER [3], making ^3He one of the standard working gases for this future machine, examining scenarii involving this gas is important. The ^3He ion being more massive than the H nucleus, RF heated ^3He ions have a lower velocity than H tails for a given RF power density and favor indirect heating of bulk ions rather than electrons. Moreover, JET is equipped with gamma ray diagnostics allowing the study of the spatial and energy distribution of fast ^3He populations [4]. Finally, mode conversion in ^3He plasmas gives rise to narrow electron power deposition profiles and thus constitutes a tool for perturbative transport studies relying on a well localized heat source.

The present paper is structured as follows: First, a few dedicated minority heating experiments are discussed. Before proceeding to a survey of the mode conversion experiments in L-mode, H-mode and ITB plasmas, the methods used to estimate the experimental power deposition profile as well as the real time control scheme set up to guarantee keeping the concentration constant are subsequently commented on. After discussing some of the results obtained at large concentration, conclusions are drawn.

2. MINORITY HEATING EXPERIMENTS

A number of ICRF physics experiments have been carried out using ^3He minority heating. Gamma ray spectrometry and tomography were key diagnostics in these experiments.

RF heating of a small minority gives rise to a subclass of highly energetic ions that slow down on electrons rather than ions. This scheme therefore does not optimally use auxiliary power to boost the ion temperature and enhance fusion reactivity. Reducing the local power density reduces the tail energy and alleviates this deleterious effect. One way of doing so is using multiple frequencies simultaneously. JET polychromatic excitation experiments, using 37MHz and 33MHz while fixing the magnetic field at 3.7T, were compared to monochromatic excitation experiments at 37MHz in (^3He)-D plasmas [5]. RF heated energetic ions have perpendicular energies significantly exceeding their parallel energy and thus tend to have trapped orbits. On account of their energy, these trajectories can have an appreciable radial extent that gives rise to exotic bean- or potato-shaped orbits. Gamma emission tomography allowed visualizing the different orbit topology when wave power was changed and/or mono- or polychromatic excitation was used. For high power and minority absorption in the center or on the low field side, a larger fraction of trapped particles and lower tail temperatures were observed for polychromatic than for monochromatic excitation. Nonstandard passing potato orbits were observed in the latter case. The SELFO code was adopted to confront theoretical and experimental findings, and allowed to demonstrate that various important aspects of minority heating (e.g. fast ions content) are within the reach of present-day theory [6].

As externally launched RF waves can reach the core of large, dense plasmas, RF heating is likely to play a role in the control of future machines of the ITER type. Since rotation impacts on plasma stability and confinement, the potential of RF induced momentum/torque transfer was looked into on JET. Toroidal rotation profiles, both when symmetric and asymmetric antenna spectra were used, were obtained via charge exchange spectroscopy [8]. The observed bulk ion rotation was found to be affected by the presence of energetic RF heated ^3He minority ions [7]. In particular, differences in toroidal rotation between discharges with $+90^\circ$ and -90° phasings were found to be consistent with absorption of wave momentum and its subsequent transfer from the fast ^3He minority ions to the background thermal plasma. Line integrated gamma ray emission revealed different radial profiles for the 2 phasings. The interpretation is that trapped ions dominate the fast ion population for -90° phasing and that a significant fraction of the heated ions are on passing orbits in the potato regime for $+90^\circ$.

As various nuclear reactions involving fast ^3He give rise to gamma ray emission, the gamma ray diagnostics available at JET provide important information on the presence of RF induced fast ^3He populations. Figure 1 shows the gamma ray yield of the 17MeV gamma rays produced in the reaction $\text{D}(^3\text{He}, \gamma) ^5\text{Li}$ as a function of time for 3 discharges with differing ^3He concentrations during which RF heating was applied. Only in the presence of RF power are fast ^3He ions observed. In agreement with theory, more very energetic RF heated ^3He particles are present (and more gamma rays are emitted) at low concentrations than at concentrations for which mode conversion is significant.

3. FAST FOURIER TRANSFORM AND BREAK IN SLOPE ANALYSIS

Knowledge of the experimental power deposition profile is the key to understanding how a heating mechanism works. By studying the ion or electron temperature response to modulation of the RF power, the (direct or indirect) power deposition profile of RF heating scenarii can be checked. The Fast Fourier Transform (FFT) technique is a powerful tool to study the response of a system to a periodic perturbation. The Break In Slope (BIS) method requires only a step change in the power level to estimate the temperature response. JET is equipped with a 96-channel electron cyclotron emission diagnostic with high temporal resolution providing detailed information on the electron temperature. FFT and BIS analysis rely on this detailed information to estimate the power deposition [9]. Both methods assume transport processes occur on a time scale much longer than the modulation period, a condition that is not fully fulfilled and can be dealt with in the frame of a full transport analysis, as the one presented later. As no detailed experimental data is available of the temporal evolution of the density, it was assumed that this quantity does not respond to the rapid changes of the modulated RF power. The momentary change of the RF power from one level to another then gives rise to a break in the slope of the temperature:

$$\frac{3}{2} kN\Delta \frac{\partial T}{\partial t} = \Delta P_{RF}$$

Whereas the BIS analysis assumes the response of the temperature to the power level change is immediate at every location, the FFT allows to track the phase lag between the moment of the power level drop or rise and the associated break in the temperature slope. The advantage of the BIS is that it can be performed at any single moment the RF power level changes, but its drawback is that, due to the non-smoothness of the measured temperature signal, the estimate of the temperature slope has significant error bars. By subtracting a time-smoothed temperature from the raw temperature data, and by subsequently folding the data points from several periods on top of one another rather than only using the data points of a single period, the BIS error bars can be reduced.

4. REAL TIME CONTROL OF THE ^3HE CONCENTRATION

Mode conversion heating in (^3He)-D plasma gives rise to localized power deposition close to the ion-ion hybrid layer. As both the efficiency of the wave conversion and the location at which it

takes place depend on the concentration, the ability to maintain the ^3He concentration (at 15-20%) is of uttermost importance. As ^3He gas is lost through transport, keeping the concentration at a specific level requires puffing extra ^3He gas into the machine during the discharge [10]. A robust way to do this is by setting up a real time control (RTC) scheme linking a measurement of the ^3He density to the opening of the gas injection valve. Such a scheme was successfully tested during the recent mode conversion experiments. Carbon is the main impurity in JET. Assuming it is the only one and making use of charge neutrality one finds that

$$\frac{N_{^3\text{He}}}{N_e} = \frac{6-Z_{\text{eff}}}{5 \frac{N_D}{N_{^3\text{He}}} + 8}$$

in which Z_{eff} is the effective charge. The relative density of the majority and minority ions is measured via the respective light in the divertor. The real-time control was developed in three stages. First, the observed open-loop response of the ^3He concentration to gas introduction was modeled using a 2nd order transfer function. Secondly, closed loop simulations of a PID control and the ^3He model were performed to tune the PID parameters. Finally, the PID controller was implemented in the Real-Time Central Controller (RTCC) system. Good control of the ^3He concentration was achieved in several pulses with different target concentrations. Figure 2 shows an example, the top figure depicting the target concentration as well as the measured concentration and the bottom figure showing the required gas puff. For diagnostic purposes, the gas puff was inhibited in various time intervals. Figure 3 depicts electron power deposition profiles at 3 different times obtained via FFT for a shot during which the magnetic field was ramped up. The RTC scheme keeps the concentration constant. Hence, the displacement of the location of the maximum of the absorption – close to the mode conversion layer – is solely due to the change of the magnetic field.

5. MODE CONVERSION HEATING

Building on earlier obtained experience [10], mode conversion experiments were performed in L-mode, H-mode and ITB plasmas. The electron temperature response to a 15Hz modulation of the RF power was studied via FFT and BIS analysis. Figure 4 shows a power deposition profile as a function of the major radius for an L-mode shot. The crosses give the BIS prediction, while the circles give the amplitude of the FFT response at the modulation frequency. The FFT and BIS analysis are in good agreement. The peak power density is of order 0.02MW/m^3 per MW launched. Integrating over the profile, one finds about 60% of the power is absorbed by the electrons.

Mode conversion experiments in H-mode were performed by adjusting the neutral beam power to ensure having grassy type III Edge Localized Modes (ELMs), the characteristic time scale of which is very short compared to the period of the modulation. The adopted power levels typically were $P_{\text{NBI}} = 14.6\text{MW}$ and $P_{\text{RF}} = 3\text{MW}$. On account of the ELMs and their impact on coupling, the temperature response shows fine structure. In spite of that, the quality of the FFT/BIS data is good on account of the different time scales.

L- and H-mode power deposition profiles obtained with FFT/BIS analysis have a very similar shape. They only represent the actual absorption profiles in a few cases, however: (i) in absence of transport and losses, or (ii) if the period of the modulation is much shorter than the time scale on which these processes take place. The drawback that the actual deposition cannot be observed becomes an advantage if one intends to perform a transport analysis: Mode conversion allows depositing power in a narrow region near the mode conversion layer and thus provides a well-localized heat source. Perturbative electron heat transport studies rely on such a heat source as they examine the heat waves propagating away from the source for a given, assumed, transport model. Adjusting the free parameters in such a model to minimize the differences between the predicted response of the harmonics for a localized source and the actual FFT response yields an estimate for the local diffusivity. It makes mode conversion heating a tool for transport analysis. Figure 5 shows the result of such an analysis for the L- and H-mode mode conversion shots using a stiffness transport model having 3 free parameters to model the diffusivity throughout the plasma [11,12]: (i) κ_{crit} , the critical inverse temperature gradient length above which turbulent transport is triggered, (ii) χ_o which, up to a gyro-Bohm-like multiplicative factor, is the background electron heat diffusivity, and (iii) χ_s which accounts for the enhanced transport when the threshold κ_{crit} has been exceeded:

$$\chi_T = q^{3/2} \frac{T}{eB} \frac{\rho}{R} [\chi_s (-R \frac{\partial T/\partial r}{T} - \kappa_{crit}) H(-R \frac{\partial T/\partial r}{T} - \kappa_{crit}) + \chi_o].$$

The dots in the figure correspond to the time averaged temperature gradient and heat flux. The small dots correspond to shots in which ion heating dominates ($T/T_i \leq 1$) while the encircled dots represent shots in which electron (mode conversion) heating is dominant ($T/T_i \geq 1$). The lines indicate the fit to modulation data. Each line corresponds to a single set of ($\chi_o, \chi_s, \kappa_{crit}$) values for which the model's prediction of the T_e response (amplitude and phase) agrees satisfactorily well with the experimental findings. The plot shows that JET electron transport is rather stiff in ion heating dominated plasmas and is less stiff for weak ion heating. It is important to note that this result relies crucially on the use of modulation, because steady-state data alone do not allow to resolve the different degrees of stiffness.

The influence of the position of the mode conversion layer on global confinement in the L-mode mode conversion shots was studied by Lysoivan [13].

Electron internal transport barriers (ITBs; see e.g. [14,15]) are formed using lower hybrid preheat in the low density startup phase of a discharge. Strong barriers are usually associated with reversed q-profiles favored by the slow penetration of the current in low density plasmas. In this phase, both the magnetic field and plasma current are being ramped up slowly. Adding NBI and RF power when the density is higher creates ion ITBs. The detailed physics of ITBs is still not fully understood but the safety factor, and via that parameter any mechanism that influences the evolution of the current, is recognized to be a key ingredient in their creation and sustainment. Like lower hybrid heating and current drive, mode conversion acts upon electrons and thus affects the electron

temperature (slowing down the current diffusion) and influences the current. As in previous experiments [10], the ^3He puff was gradually increased from discharge to discharge to monitor the transition from minority to mode conversion heating. It was observed that strong ITBs can be formed and maintained when RF heating is located inside the ITB. These shots are characterized by reversed q-profiles and by high central temperatures. High ion and electron temperatures (up to, respectively, 25keV and 13keV) were recorded at ^3He concentrations well beyond those optimal for minority heating. Figure 6 shows an example.

Figure 7 summarizes the performance of the recent ITB plasma experiments (full circles) together with the other shots in the JET advanced scenario data base. The recent data points are underlining the efficiency of this heating scheme. At any auxiliary power level, the ion and electron temperatures attained in many of the recent ITB shots, for which $N_{3\text{He}}/N_e > 10\%$, are among the highest ones achieved.

CONCLUSIONS

Recent ^3He experiments in JET included studies of RF induced rotation, a performance comparison of mono- versus polychromatic excitation and an extensive mode conversion study. Mode conversion was adopted as a transport tool to demonstrate the stiffness of core electron transport both in JET L- and H-mode. Fine-tuning the mode conversion tool involved the successful development of a real time control scheme of the ^3He concentration.

REFERENCES

- [1]. Stix, T.H., Waves in Plasmas, New York: AIP, 1992
- [2]. Perkins, F.W., Nucl. Fusion **17**, 1197-1224 (1977)
- [3]. Van Eester, D. , et al., Nucl. Fusion **42**, 310-328 (2002)
- [4]. Kiptily, V., et al., Nucl. Fusion **42**, 999-1007 (2002)
- [5]. Mantsinen, M., et al., "Comparison of monochromatic and polychromatic ICRH on JET", this conference
- [6]. Laxaback, M., et al., "Self-consistent modeling of polychromatic ICRH", this conference
- [7]. Eriksson, L.-G., et al., "Bulk Plasma Rotation in presence of waves in the ion cyclotron range of frequencies", this conference
- [8]. J.-M. Noterdaeme, et al., Nuclear Fusion **43**, 274-289 (2003)
- [9]. Gambier, D.J., et al., Nucl. Fusion **30**, 23-34 (1990)
- [10]. M. Mantsinen, et al., "Localized bulk electron heating with ICRF mode conversion in the JET tokamak", JET-EFDA paper EFD-P(03)21, submitted to Nuclear Fusion
- [11]. Mantica, P., et al., "Transient heat transport studies in JET conventional and advanced tokamak plasmas", Fusion Energy 2002 (Proc. 19th Int. Conf. Lyon, 2002), EX/P1-04, IAEA, Vienna.
- [12]. Mantica, P., "Heat wave propagation experiments and modeling at JET: L-mode, H-mode and ITBs", to be presented at the 2003 EPS conference, St.Petersburg

- [13]. Lyssoivan, A., et al., “Effect of ICRF mode conversion at the ion-ion hybrid resonance on plasma confinement in JET”, this conference
- [14]. Joffrin, E., et al., “Internal transport barrier triggering by rational magnetic flux surfaces in tokamaks”, submitted to Nuclear Fusion
- [15]. Mazon, D., et al., “Real-time control of internal transport barriers in JET”, submitted to Plasma Phys. Contr. Fusion

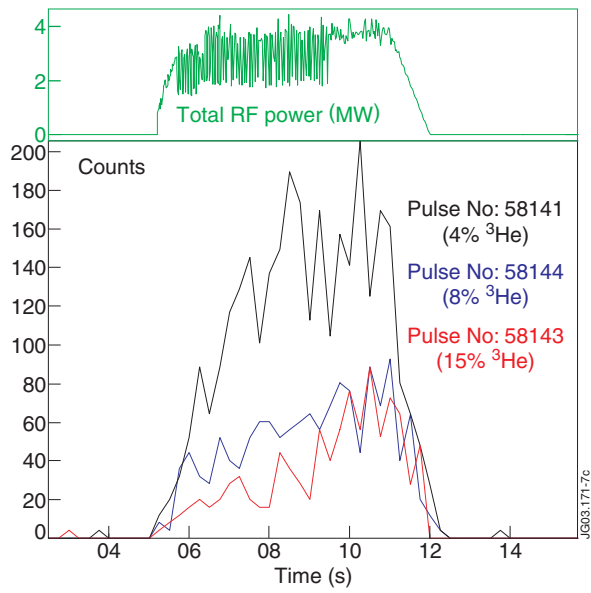


Figure 1: RF power (top) and gamma ray emission (bottom) for 3 shots with different ^3He concentrations.

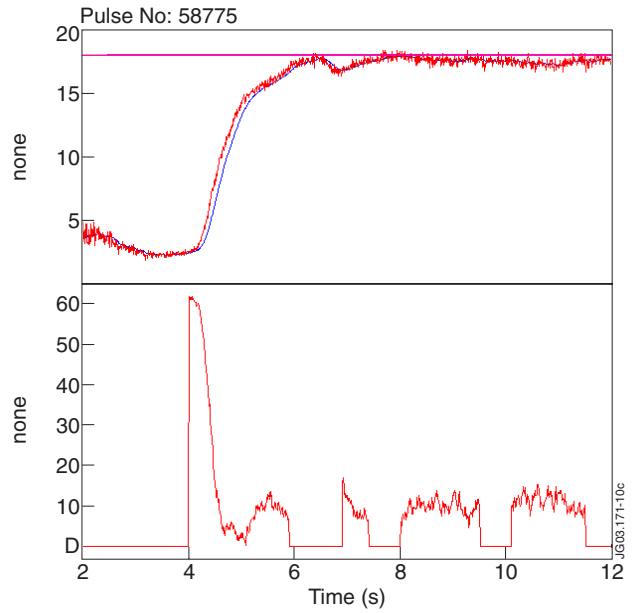


Figure 2: Real time control of the ^3He concentration: requested & validated concentration (top) and valve opening (bottom).

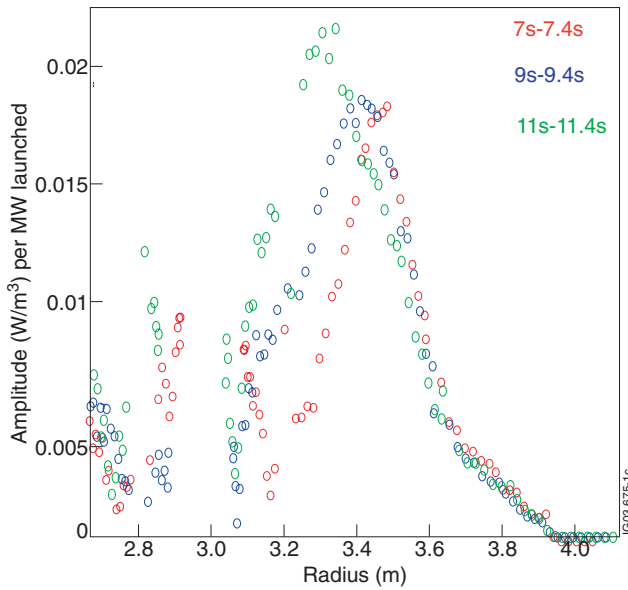


Figure 3: Moving the electron power deposition maximum by changing the magnetic field.

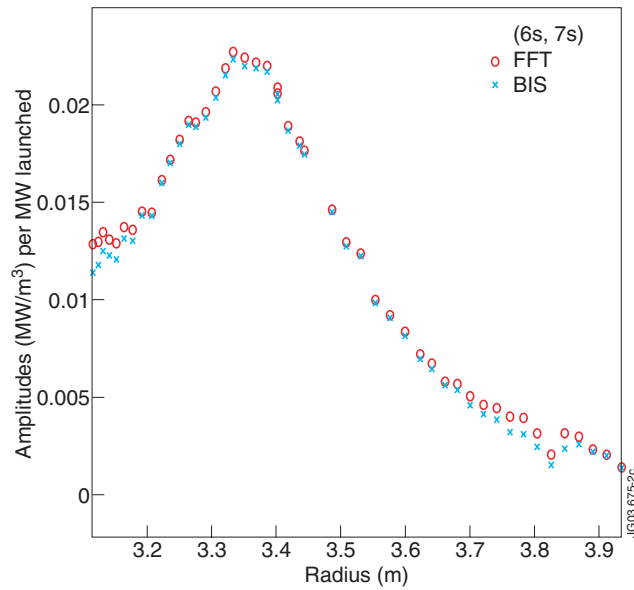


Figure 4: L-mode power deposition profile from FFT/BIS

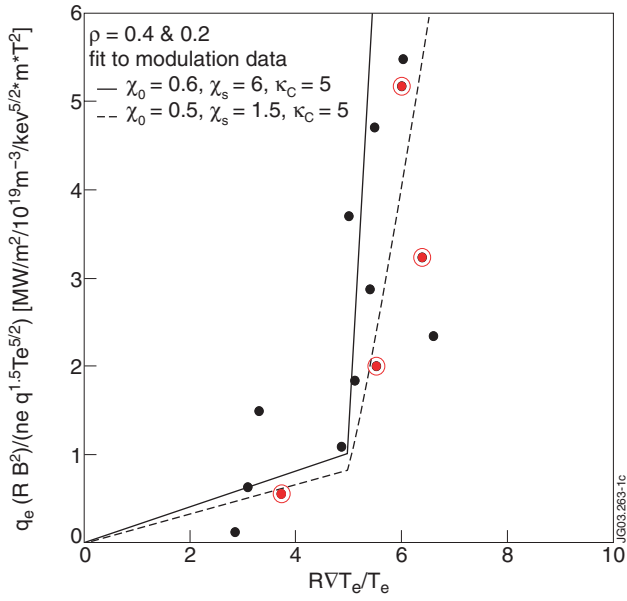


Figure 5: Normalized e heat flux as a function of the inverse temperature gradient length.

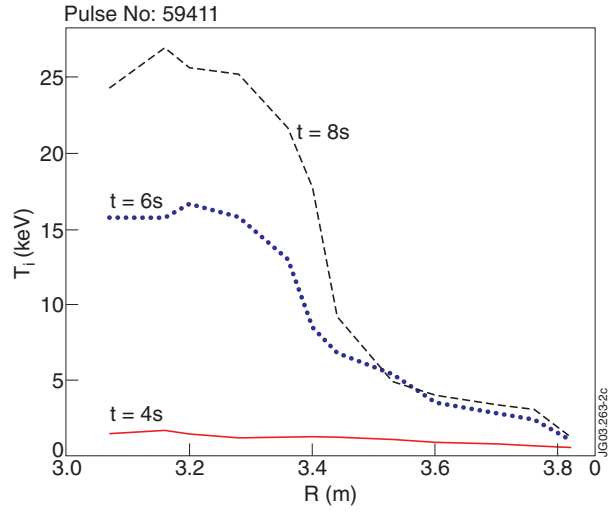


Figure 6: Ion temperature profile of an ITB shot.

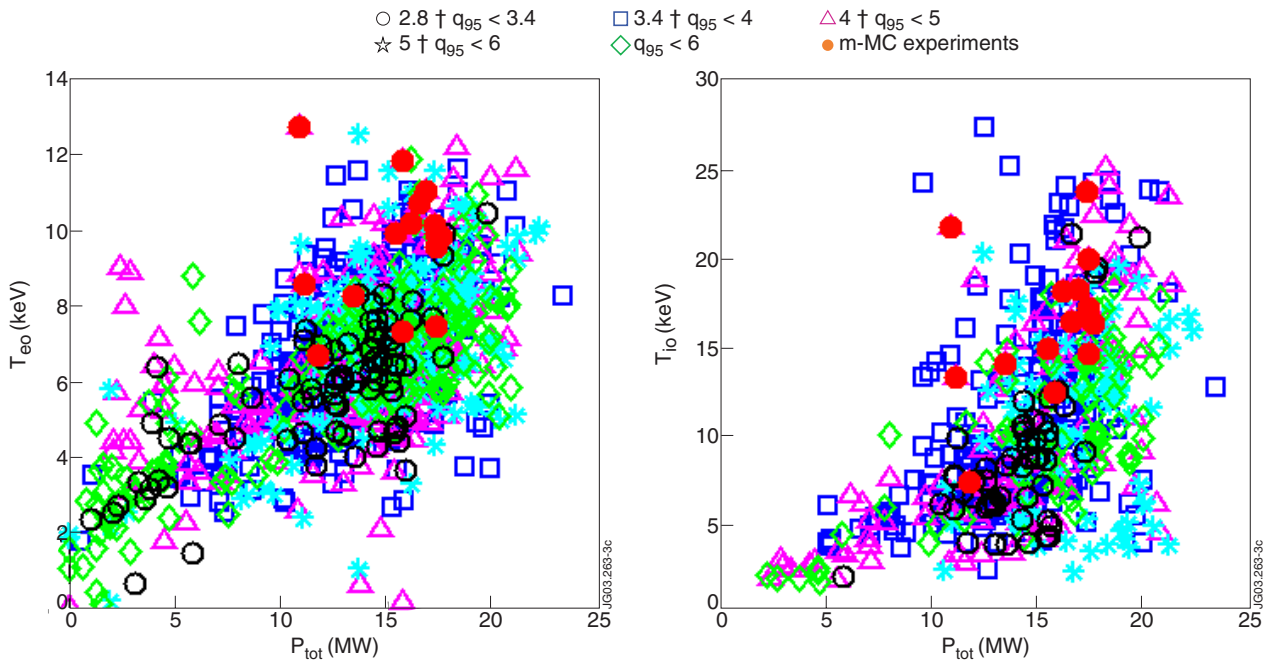


Figure 7: Performance of recent m-MC heating ($N_{3He} / N_e > 10\%$) and earlier ITB shots